Modeling Large-Area Influence in Digital Halftoning for Electrophotographic Printers*

Yanling Ju[a], Dhruv Saxena[a], Tamar Kashti[b], Dror Kella[b],
Doron Shaked[c], Mani Fischer[c], Robert Ulichney[d], and Jan P. Allebach[a]

[a]School of Electrical and Computer Engineering, Purdue University,
West Lafayette, IN 47907-2035, U.S.A.
[b]Hewlett-Packard Indigo, Ltd. Ness Ziona, Rehovot, 76101, ISRAEL
[c]Hewlett-Packard Laboratories Israel, Technion City, Haifa, 32000, ISRAEL
[d]Hewlett-Packard Laboratories USA, Cambridge, MA 02142 , U.S.A.

ABSTRACT

Digital halftoning provides a mechanism for rendering continuous-tone images on devices such as printers. With electrophotography, the deposition of toner within the area of a given printer addressable pixel is strongly influenced by the halftone values of the immediately neighboring pixels. To account for these effects, it is necessary to embed a printer model in the halftoning algorithm.

In our previous work, we used an efficient strategy to account for the impact of a 5×5 neighborhood of pixels on the central pixel absorptance. Now we examine the potential influence of a much larger neighborhood (45×45) of the digital halftone image on the measured value of a printed pixel at the center of that neighborhood. The experiment shows that the extended model yields a significant improvement in the accuracy of the prediction of the pixel values of the printed and measured halftone image.

Keywords: Digital halftoning, printer models, electrophotography, least squares regression

1. INTRODUCTION

Digital halftoning is the process of representing a continuous-tone image with a device that can render only two or a few different levels of absorptance. Since the human visual system (HVS) acts as a spatial low-pass filter, which can blur the rendered halftone image, the halftone image can be perceived as a continuous-tone image.

Traditional halftoning algorithms assume that there is no interaction or just additive ones between neighboring dots. That means the absorptance of a printed binary pattern is linearly proportional to the number of black dots printed on the paper. But this is not true for real printers. Under this assumption, the printed image is often darker than expected. This phenomenon is called dot gain and it is nonlinear. Dot gain can be caused by one or all of the following effects: optical (trapping of scattered light under the colorant), mechanical (spreading of colorant on the medium), and electric fields (only for electrophotographic (EP) printers). Several approaches have been taken to account for this nonlinear behavior.[1] One approach is to use clustered-dot textures. Clustered-dot screens are very suitable for the printing processes that cannot render stable isolated dots. But they result in visible dot texture and loss of detail because the clustered-dot halftone textures have more energy at lower frequencies. The second approach is to use tone correction. This gives correct average tone but does not give good detail rendition. The third approach is to use a printer model within the halftoning algorithm.[2]

Among the different derived printer models, the most commonly used is the hard circular dot (HCD) printer model. The HCD model assumes that the shape of the black dots produced by a printer is a circular spot with constant absorptance, and multiple dot overlap is resolved by a logical OR.[3–9] The HCD model was first used to modify the ordered dither thresholds to ensure linear gray scale by Roetling and Holladay.[3] Allebach[4] took into account the effect of neighboring dots on texture and proposed a modification to ordered dither that accounts for local dot interaction at the expense of spatial resolution. Stucki[6] and Stevenson[5] also proposed some enhancements to error diffusion that incorporate a HCD model. Pappas et al.[8,9] parameterized the HCD

* This work was supported by the Hewlett-Packard Company.

model, characterizing local dot interaction by three variables and applied the HCD model to several halftoning techniques, including the iterative least squares algorithm. But at higher resolutions, the HCD model will not accurately predict the microstructure of dots printed with the EP process.[2]

The stochastic printer model is also a type of commonly used printer model.[2,10–12] Lin and Wiseman[10] proposed the use of a stochastic printer model for an EP printer that is based on a probability density function to model the random placement of toner particles on a microlattice. Flohr and Allebach[12] used it to improve DBS textures. Unfortunately, incorporating these stochastic models within the DBS algorithm is computationally very expensive. Moreover, the efficacy of these methods is dependent on how well the probability density function models the actual printer behavior.

Most of the above mentioned approaches assume a logical OR at dot placement locations to resolve the multiple dot overlap. This is an ideal assumption that does not hold for most printers. The actual printed result may differ substantially from that which might be expected based on the bitmap generated by the halftoning algorithm. The nature and source of these differences will vary depending on the marking technology –be it electrophotography or inkjet, and the specific characteristics of the print mechanism. With electrophotography, the deposition of toner within the area of a given printer-addressable pixel is strongly influenced by not just the halftone value at that pixel, but also by the halftone values of the immediately neighboring pixels. This local influence can be attributed to the fact that the spot size of the laser write beam is larger than a single printer addressable pixel; the complex field interactions that are set up by the charge distribution on the photoconductor and in the toner in the gap between the photoconductor and the developer, and how this influences development; the further spreading of toner during the transfer and fusing processes; and optical scattering of incident light within the media.

In our previous research[2] on the model for electrophotographic printers, we used a 3×3 LUT to account for these interactions, and populated that table with data based on microanalysis of an exhaustive set of possible printed 3×3 binary halftone patterns. More recently, we presented an efficient strategy to estimate the impact of 5×5 neighborhood pixels on the central pixel absorptance, by using the same LUT based approach as before to exhaustively represent the influence of the inner 3×3 neighborhood, while summarizing the influence of the outer 5×5 outer pixels by forming a weighted sum of these halftone pixels.[13]

In the present paper, we examine the potential influence of a much larger neighborhood of the digital halftone image on the measured value of a printed pixel at the center of that neighborhood. This influence is believed to be due to the scattering of light within the media, rather than the other factors mentioned above. Our target device in this work is the HP Indigo Press 5000, but the results should be broadly applicable to all electrophotographic printers. We first print and analyze a set of test patterns that use a stochastic, dispersed-dot digital halftone texture as the outer neighborhood and analyze the influence of that neighborhood on the absorptance value of the center pixel. These results show that it is possible to account for the influence of this larger neighborhood with a function of only the average absorptance value of the digital halftone image within the larger neighborhood. As a conservative estimate of the size of this larger neighborhood, we take it to be a 45×45 region of 1/812.8 × 1/812.8 in^2 printer addressable pixels for the Indigo press. The functional form that maps the average gray value of the outer $45 \times 45 - 5 \times 5$ neighborhood to its contribution to the measured value of the center pixel is the same as that used to model the influence of all the pixels in the 5×5 inner neighborhood. However, the parameterization is based on printing and measuring a different set of test patterns than were used to capture the influence of the inner 5×5 neighborhood. Finally, we show that the extended model yields a significant improvement in the accuracy of the prediction of the pixel values of the printed and measured halftone image for stochastic, dispersed-dot halftone textures.

The remainder of the paper is organized as follows. Section 2 describes the notation used in this paper and printer models. Then in Section 3, we discuss in detail the stochastic printer models that we have developed. Experimental results are presented in Section 4. Finally, conclusions are drawn in Section 5.

2. PRELIMINARIES

2.1 Notation

We use $[x, y]$ for continuous spatial coordinates and $[m, n]$ for discrete spatial coordinates. The units of $[x, y]$ and $[m, n]$ are inches and pixels, respectively. The function $g[x, y]$ denotes the continuous-tone image, and $g[m, n]$

denotes the digital halftone. For each pixel of $g[m,n]$, the absorptance values can only take on values of 0 (white) or 1 (black).

2.2 Printer models

Prnter models can be embedded into the halftoning algorithm to try to get a more accurate result. Algorithms that have some model for the printing process assume either linear or nonlinear dot interaction. Most printer models assume the interaction between neighboring dots is additive. In that case, the rendered halftone can be expressed in terms of the digital halftone and the printer spot profile

$$g_r(x,y) = \sum_{m,n} g[m,n]p(x - mX, y - nX), \tag{1}$$

where $p(x,y)$ is the spot profile function of the ideal printer and X is the distance between addressable pixels. The perceived halftone is then given by

$$\tilde{g}_r(x,y) = \sum_{m,n} g[m,n]\tilde{p}(x - mX, y - nX), \tag{2}$$

where

$$\tilde{p}(x,y) = p(x,y) * *h(x,y). \tag{3}$$

But as mentioned above, this model is not true for real printers. For example, for electrophotographic printers, the deposition of toner within the area of a given printer-addressable pixel is strongly influenced by not just the halftone value at that pixel, but also by the halftone values of the immediately neighboring pixels. This means that the developed toner mass at any point in the image is a nonlinear function of the halftone in the neighborhood of that point. The nonlinear term may be caused by several phenomena: a) overlap of the Gaussian laser beam used to write the latent image on the organic photo-conductor (OPC); b) field effects during development; and c) toner particle displacement and distortion during transfer and fusing. A critical concept is the equivalent grayscale image $\hat{g}[m,n]$ which summarizes dot gain effects by a single value in the rendered halftone that is constant over each entire $X \times X$ printer addressable pixel.[2]

2.2.1 Model-3×3

There are 512 (2^9) different 3×3 dot patterns. To ensure the full characterization of the printing press for Model-3×3, we design test pages that include all 512 different dot patterns; print the test pages on the HP Indigo Press 5000 at resolution 812.8 dpi; scan the printed images using an Epson Expression10000 XL scanner at resolution 2400 dpi; and analyze the scanned test pages to estimate the mean and standard deviation of the central pixel absorptance of each 3×3 dot pattern. Specifically, our estimate of the mean and standard deviation of the absorptance of the central pixel of each 3×3 dot pattern is given by the sample mean and sample standard deviation of the corresponding scanned dot patterns. We store these estimated values in a lookup table (LUT).

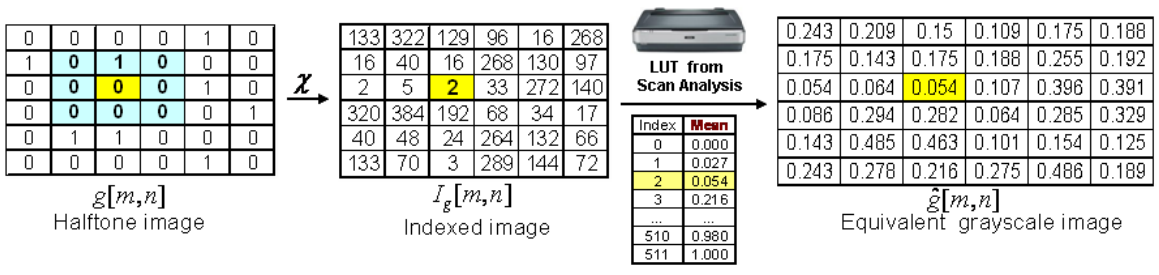

Figure 1. Using Model-3×3 to generate the equivalent grayscale image.

The lookup table (LUT) is the stochastic model-3×3. We will use this model to generate both an equivalent grayscale image and the sample variance of this image. Figure 1 shows how to use the model to generate the equivalent grayscale image. The procedure for generating the sample variance image is similar.

2.2.2 Model-5×5

We use a similar approach to generate the Model-5×5. Since the number of all possible 5×5 dot profiles is 2^{25}, it is impossible to print all 5×5 dot configurations. To develop a feasible approach, it is assumed that dots in the outer ring of the 5×5 neighborhood have an additive influence on the central pixel absorptance. We consider all 512 3×3 inner dot configurations, and then randomly choose a set of M different 5×5 outer dot configurations as the training set.

We use the least squares method to find the optimal weights for each of the 16 dots in the outer ring of the 5×5 neighborhood. The additive contribution of the dots present in the outer ring of the 5×5 neighborhood can be computed using the optimal weights. For the unbiased linear model,

$$\lambda_{i,j} = \lambda_{i,0} + \Psi_j^T W_i + c_i, \tag{4}$$

where i is the index of 3×3 dot configuration, j is the index of 5×5 outer dot configuration, Ψ_j denotes the 16×1 vector corresponding to the j^{th} binary 5×5 outer dot configuration in the training set, W_i denotes the 16×1 weight vector that characterizes the additive influence of dots in the outer ring of the 5×5 neighborhood on the central pixel mean absorptance of the i^{th} 3×3 dot configuration, c_i is a constant term that corrects for model bias, $\lambda_{i,j}$ is the central pixel mean absorptance of the i^{th} 3×3 dot configuration with the j^{th} 5×5 outer dot configuration, and $\lambda_{i,0}$ is the central pixel mean absorptance of the i^{th} 3×3 dot configuration without considering the contribution of the 5×5 outer ring. The equation for the equivalent grayscale image is

$$\hat{g}[m,n] = \Omega_{model}\{g[m+k, n+l], (k,l) \in [-2:2]^2\}, \tag{5}$$

where $[-2:2]^2$ denotes the 25 point set of 2-tuples formed by the cartesian product of $[-2:2]^2$ with itself, and Ω denotes the transformation of the binary value to the equivalent grayscale value of the center pixel.[13] The procedure for generating the sample variance image is similar.

3. NEW PRINTER MODEL TO ACCOUNT FOR LARGE-AREA INFLUENCE

In this section, we describe the print-to-scan analysis procedure that is used for modeling large-area influence in digital halftoning and how the estimates are used to develop the stochastic model for the HP Indigo Press 5000. The printer has a resolution 812.8 dpi. After printing the test pages, the printed images are scanned using an Epson Expression 10000 XL scanner at resolution 2400 dpi.

3.1 Print-to-Scan Analysis Procedure

The stochastic printer models are developed for the HP Indigo Press 5000. As an electrophotographic printer, as we discussed above, the printed dot is not round and solid black but a random distribution of colorant at a higher resolution. We assume that conditioned on the average absorptance within each $X \times X$ cell, the distribution of toner particles that get transferred is random and uncorrelated from $X \times X$ cell to $X \times X$ cell. The printer model developed by Goyal[13] calculates the absorptance of a pixel using its 5×5 neighborhood. We expand the model to incorporate the effect of a neighborhood greater than 5×5 by taking into account the influence of a 45×45 neighborhood on the central pixel absorptance. First, we use the print-to-scan analysis to build the Model-5×5, then use the similar strategy to estimate the influence of the $45 \times 45 - 5 \times 5$ neighborhood on the central pixel absorptance. The estimated central pixel absorptance of Model-45×45 is the sum of the estimated central pixel absorptance of Model-5×5 and the additive influence of the $45 \times 45 - 5 \times 5$ neighborhood on the central pixel absorptance.

3.1.1 Building Model-5×5

We design test pages that include all the 512 different inner 3×3 dot patterns and 160 different 5×5 outer neighborhoods. there are $512 \times 160 = 81,920$ different 5×5 dot patterns. Each 5×5 dot pattern is replicated 50 times to average out the inherent printer instability. Altogether, we have six test pages with each page containing $86 \times 160 \times 50 = 688,000$ patterns. To solve the alignment problem, each 3×3 group of nine 5×5 dot patterns is surrounded by four fiducial marks. The distance between the fiducial marks is set to be large enough to ensure that the fiducial marks do not influence the dot development of the 5×5 dot pattern. Figure 3 (a) shows a

portion of such a test page. We print the test pages on the HP Indigo Press 5000 at resolution 812.8 dpi, and scan the printed images using an Epson Expression10000 XL scanner at resolution 2400 dpi. We analyze the scanned test pages to estimate the mean and standard deviation of the absorptance of the central pixel. To analyze the scanned test pages, we first perform scanner gray balancing to calibrate the scanned image to units of absorptance. Each scanned image is binarized by Otsu's method[14] to generate a corresponding binary mask for the fiducial marks. The centroid of each fiducial mark is calculated based on the spatial distribution of toner absorptance throughout its corresponding mask region. Let D_i be the segmented region of the i^{th} fiducial mark in the binary mask image. Then, the horizontal and vertical centroids of the i^{th} segmented fiducial mark are given by

$$C_{x,i} = \frac{\sum_{[m,n]\in D_i}(m-0.5)A[m,n]}{\sum_{[m,n]\in D_i}A[m,n]}, C_{y,i} = \frac{\sum_{[m,n]\in D_i}(n-0.5)A[m,n]}{\sum_{[m,n]\in D_i}A[m,n]} \tag{6}$$

where $A[m,n]$ is the absorptance value of the scanned image at the pixel with coordinates $[m,n]$.

The center of the dot pattern can be computed using the estimates of the centroids of the fiducial marks. Next, we use this center to calculate the absorptance of the $2400/812.8 \times 2400/812.8$ scanned pixels that correspond to the central pixel of the printed dot pattern. The estimates of the mean and standard deviation of the absorptance of the central pixel of each 5×5 dot pattern are given by the sample mean and sample standard deviation of the corresponding scanned dot patterns. We store the estimates of the mean and standard deviation absorptance of the central pixel of the 3×3 dot configurations without any dots in the outer 5×5 ring as a lookup table (LUT). The lookup table (LUT) is the stochastic Model-3×3.

We estimate the outer 5×5 neighborhood impact on the inner 3×3 dot configuration using the mean and standard deviation of the absorptance of the remaining 5×5 dot patterns. The whole Model-5×5 strategy is shown in Fig. 2

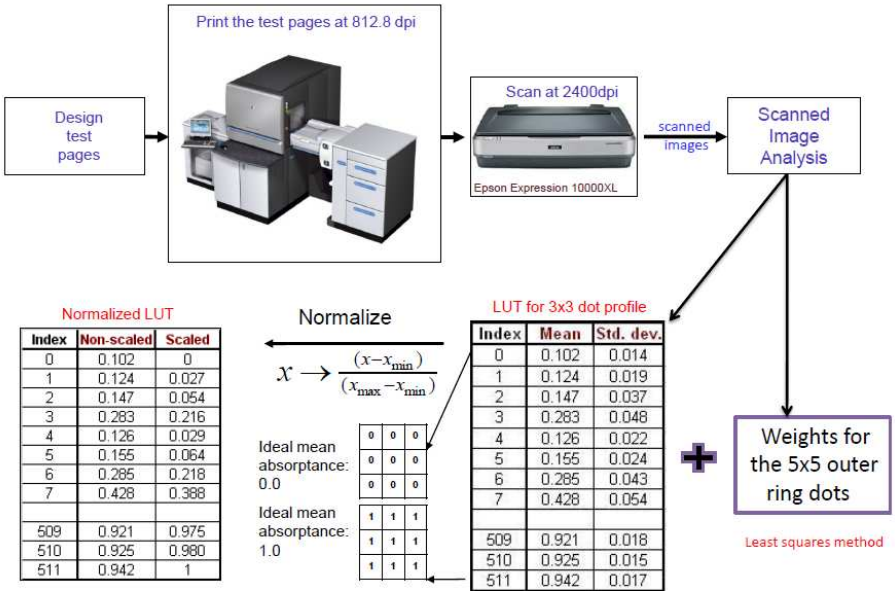

Figure 2. Model-5×5 strategy.

We assume an unbiased linear model to incorporate the influence of dots in the outer ring of the 5×5 neighborhood. The central pixel mean absorptance of any 5×5 dot configuration is the sum of the central pixel mean absorptance of the corresponding 3×3 dot configuration with no dots in the outer 5×5 ring and the additive contribution of the dots present in outer ring of the 5×5 neighborhood, which is characterized by a set of weight

parameters. Eq. (7) shows this model.

$$\begin{aligned}\lambda_{i,j}^{predicted-5\times5} &= \lambda_{i,0}^{measured-3\times3} + \psi_j^T w_i^{Model-5\times5} + c_i^{Model-5\times5}, \\ &= \lambda_{i,0}^{measured-3\times3} + \Psi_j^T W_i^{Model-5\times5},\end{aligned} \tag{7}$$

Here i is the index of the 3×3 dot configuration, j is the index of the 5×5 outer dot configuration, $\lambda_{i,j}^{predicted-5\times5}$ is the predicted central pixel mean absorptance of the i^{th} 3×3 dot configuration with the j^{th} 5×5 outer dot configuration, $\lambda_{i,0}^{measured-3\times3}$ is the measured central pixel mean absorptance of the i^{th} 3×3 dot configuration without the 5×5 outer ring, ψ_j denotes the 16×1 vector corresponding to the j^{th} 5×5 outer ring in the training set, $w_i^{Model-5\times5}$ denotes the 16×1 weight vector that characterizes the additive influence of the dots in the outer ring of the 5×5 neighborhood on the central pixel mean absorptance of the i^{th} 3×3 dot configuration, and $c_i^{Model-5\times5}$ denotes the constant offset term that removes the model bias. In the second line of Eq. (7), we absorb the constant offset term within the weight vector by augmenting ψ_j^T with a 1 to yield the 17×1 vector Ψ_j^T, and then augmenting $w_i^{Model-5\times5}$ with $c_i^{Model-5\times5}$ to yield the 17×1 vector $W_i^{Model-5\times5}$. Applying the least squares method, we obtain the optimal weights

$$W_i^{Model-5\times5} = argmin\{\Psi_j^T W_i^{Model-5\times5} - \Delta\lambda_i\}, \tag{8}$$

Thus,

$$W_i^{Model-5\times5} = (\Psi^T\Psi)^{-1}\Psi^T\Delta\lambda_i, \tag{9}$$

where

$$\Delta\lambda_i = \left[\lambda_{i,1}^{measured-5\times5} - \lambda_{i,0}^{measured-3\times3}, ..., \lambda_{i,M}^{measured-5\times5} - \lambda_{i,0}^{measured-3\times3}\right]. \tag{10}$$

Here, $\lambda_{i,j}^{measured-5\times5}$ denotes the measured central pixel absorptance value for the i^{th} dot configuration in the inner 3×3 region and the j^{th} dot configuration in the outer 5×5 ring for each of the $j = 1, ..., M$ outer configurations, averaged over the 50 printed replications of each of these 5×5 patterns. These data are used to train the weight vector $W_i^{Model-5\times5}$ for the i^{th} 3×3 dot configuration. The parameter $\lambda_{i,0}^{measured-3\times3}$ is the measured central pixel absorptance value for the i^{th} dot configuration in the inner 3×3 region without dots in the outer 5×5 ring. We used $M = 160$ in our experiments.

3.1.2 Model-45×45

For a large neighborhood, for example, in a K×K window, there are 2^{K^2} different possible dot configurations. It is impossible to print all such dot configurations to measure the absorptance of the central pixel. Hence to make the problem solvable, we first print and analyze a set of test patterns that include a stochastic, dispersed-dot digital halftone within the $45 \times 45 - 5 \times 5$ neighborhood surrounding the central 5×5 pixels region, and analyze the influence of the neighborhood on the absorptance value of the center pixel. The results show that it is possible to account for the influence of this larger neighborhood with a function of only the average value of the digital halftone image within the larger neighborhood. As a conservative estimate of the size of this larger neighborhood, we take it to be a 45×45 window of $1/812.8 \times 1/812.8$ in^2 printer addressable pixels for the Indigo press.

We now describe the procedure to calculate the mean and standard deviation of the absorptance of the central pixel for all the possible 3×3 dot patterns with a 45×45 neighborhood and how to use these estimates to develop the stochastic model. We assume that the dots in the neighborhood outside the 5×5 neighborhood have an additive influence on the central pixel absorptance. We call the percentage of the total number of dots printed in the $45 \times 45 - 5 \times 5$ neighborhood the graylevel of the neighborhood. The influence of the $45 \times 45 - 5 \times 5$ neighborhood on the central pixel absorptance is modeled as a function of only the graylevel of the digital halftone image within the $45 \times 45 - 5 \times 5$ neighborhood.

We design test pages to estimate the parameters of Model-45×45 as follows. There are 512 different inner 3×3 dot configurations. For a single randomly chosen inner 3×3 dot configuration (index = 306), we randomly choose a set of 72 different dot patterns in the outer 5×5 ring. We consider 21 different gray levels for the outer $45 \times 45 - 5 \times 5$ neighborhood. For each of these gray levels, we generate a single stochastic, dispersed-dot

halftone pattern with that average gray level. We then embed each of the 72 inner 5×5 dot patterns described above within this $45 \times 45 - 5 \times 5$ halftone pattern. This process yields a total of $21 \times 72 = 1,512$ unique binary patterns. We print each of these patterns 50 times in random order. The inner 3×3 dot configuration with index 306 corresponds to the binary pattern $[1, 0, 0; 0, 1, 1; 0, 0, 1]$. Altogether, three pages are required to print these 75,600 patterns, with each page containing 25,200 patterns. To solve the alignment problem, each dot pattern is surrounded by four fiducial marks. Figure 3 (b) shows a portion of such a test page. Those pages were printed on an Indigo Press 5000 at 812.8 dpi. Then the printed test pages were scanned on the Epson Expression 10000 XL scanner at resolution 2400 dpi.

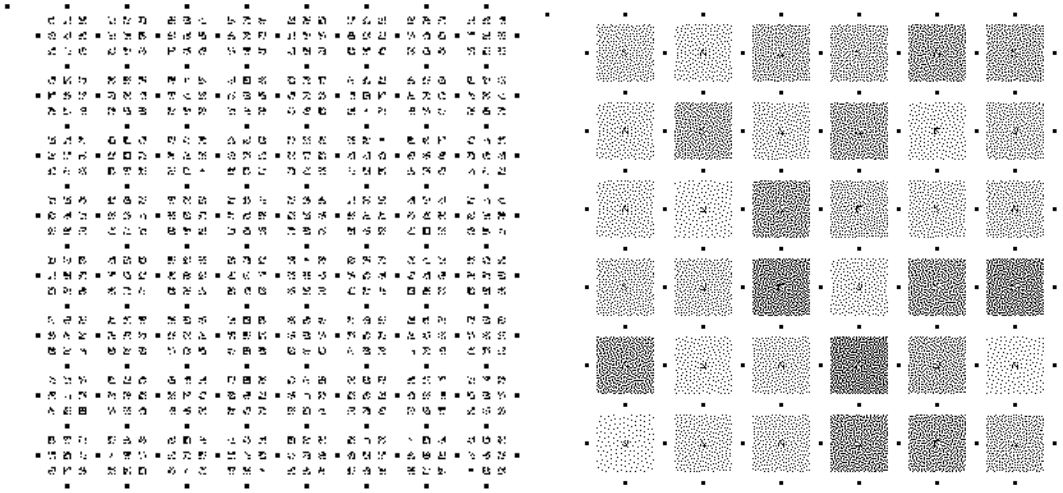

(a) (b)

Figure 3. Test pages used for model development. a) portion of a Model-5×5 test page, b) portion of a Model-45×45 test page.

We analyze the scanned test pages using a strategy similar to that for the Model-5×5 mentioned above. After we have the estimates of the mean and standard deviation of the absorptance of the central pixel of each individual 45×45 dot pattern, we build the Model-45×45 by combining the measured values with the Model-5×5 predicted values. Eq. (11) shows the structure of the model-45×45. Here, $\lambda_{i,j,g}^{predicted-45\times45}$ is the overall prediction of the central pixel absorptance for the i^{th} inner 3×3 dot configuration, the j^{th} dot configuration in the outer 5×5 ring, and gray level g for the outer $45 \times 45 - 5 \times 5$ halftone pattern. The term $\lambda_{i,j}^{predicted-5\times5}$ is the Model-5×5 predicted central pixel absorptance given by Eq. (7). The remaining terms in the two lines of Eq. (11) are analogous to the corresponding terms in Eq. (7), with the addition of dependence on the gray level g, where appropriate.

$$\begin{aligned} \alpha_{i,j,g}^{predicted-45\times45} &= \lambda_{i,j}^{predicted-5\times5} + \psi_j^T w_{i,g}^{Model-45\times45} + c_{i,g}^{Model-45\times45}, \\ &= \lambda_{i,j}^{predicted-5\times5} + \Psi_j^T W_{i,g}^{Model-45\times45}, \end{aligned} \tag{11}$$

As shown in Eq. (12) - (14), we again use a least squares approach to find optimal weights.

$$W_{i,g}^{Model-45\times45} = argmin\{\Psi_j^T W_{i,g}^{Model-45\times45} - \Delta\lambda_{i,g}\}, \tag{12}$$

$$\Delta\lambda_{i,g} = \left[\lambda_{i,1,g}^{measured-45\times45} - \lambda_{i,1}^{predicted-5\times5}, ..., \lambda_{i,M,g}^{measured-45\times45} - \lambda_{i,M}^{predicted-5\times5}\right]. \tag{13}$$

Thus,

$$W_{i,g}^{Model-45\times45} = (\Psi^T\Psi)^{-1}\Psi^T\Delta\lambda_{i,g}, \tag{14}$$

Here, $\lambda_{i,j,g}^{measured-45\times45}$ denotes the average measured central pixel absorptance value for the i^{th} dot configuration in the inner 3×3 region and the j^{th} dot configuration in the outer 5×5 ring with gray level g for the outer

$45 \times 45 - 5 \times 5$ halftone pattern. The parameter $\lambda_{i,j}^{predicted-5\times5}$ is the predicted central pixel absorptance value using Model-5×5 for the i^{th} dot configuration in the inner 3×3 region and the j^{th} dot configuration in the outer 5×5 ring. Here $j = 1, ..., M$, and we used $M = 72$ in our experiments.

4. EXPERIMENTAL RESULTS

Model-5×5 test pages were designed as Figure 3 (a). Using the print-to-scan analysis procedure for those test pages, we compute the central pixel mean absorptance for each individual 3×3 dot configuration with 160 randomly chosen different 5×5 outer dot configurations. Using these statistics, we obtain the Model-3×3 and optimal weights of the 5×5 outer dot configuration for each different 3×3 dot configuration, which is Model-5×5.

Then we use a similar analysis procedure for the Model-45×45 test pages. For each gray level represented by a fixed $45 \times 45 - 5 \times 5$ digital halftone pattern, we perform the following computation. For each of the 72 5×5 dot configurations, we compute the sample mean and variance of the measured central pixel absorptance across the 50 printed replications of the identical 45×45 digital halftone pattern. We use the sample mean absorptance to build the Model-45×45. To reflect the variability in the printing process, we then average the sample variance across all 72 different 5×5 dot configurations printed with the $45\times45-5\times5$ digital halftone pattern corresponding to this gray level. Finally, we take the square root of this result to yield the sample standard deviation.

To compare stochastic printer Model-5×5 and Model-45×45, for a fixed 3×3 dot configuration with fixed 5×5 outer dot configuration and $45 \times 45 - 5 \times 5$ outer neighborhood, we predict the mean absorptance of the central pixel using Model-5×5 and Model-45×45, respectively. The prediction error is computed as the difference between the measured mean absorptance value and the predicted mean absorptance value.

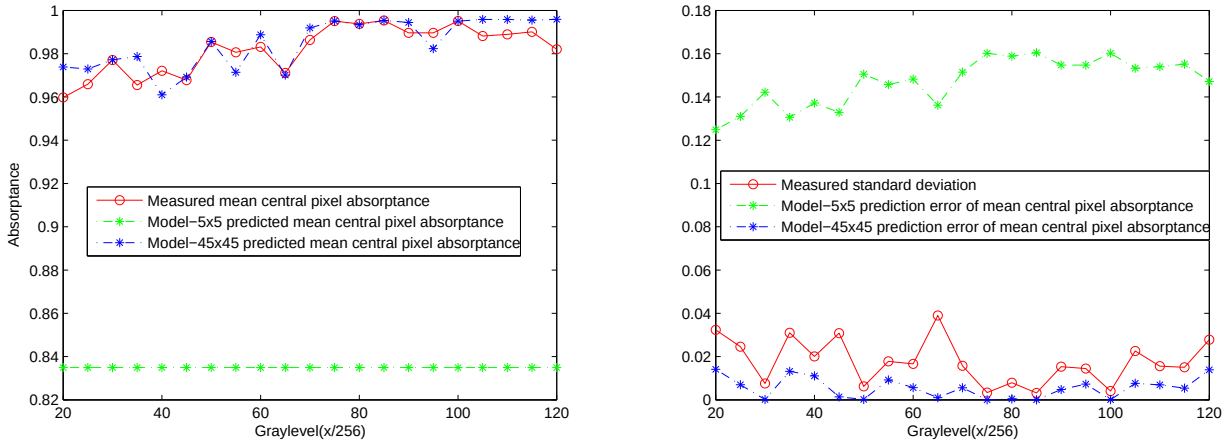

(a) (b)

Figure 4. Experimental results for the models. a) predicted mean absorptance using different models, b) prediction error of different models. To facilitate comparison with the measured standard deviation, we show the absolute value of the Model-45×45 prediction error.

In Fig. 4(a), the red curve is the measured absorptance of the central pixel averaged over all 72×50 different halftone patterns corresponding to each fixed average gray level; the green curve is the mean central pixel absorptance predicted by Model-5×5, and averaged over the 72 different halftone patterns; and the blue curve is the mean central pixel absorptance predicted by Model-45×45, and averaged over the 72 different halftone patterns. As discussed above, the inner 3×3 dot configuration for all these 45×45 patterns is $[1, 0, 0; 0, 1, 1; 0, 0, 1]$. Since the central pixel contains a printed dot that is horizontally and diagonally adjacent to three other printed dots, we expect the absorptance of the central pixel to have a relatively large value, regardless of the dot configuration in the outer 5×5 ring or the gray value of the halftone pattern in the outer $45 \times 45 - 5 \times 5$ region. This is indeed what we observe in Fig. 4(a). In Fig. 4(b), the red curve is the measured sample standard

deviation calculated as above; the green curve is the error in the prediction of the mean central pixel absorptance by Model-5 $\times$ 5, and averaged over the 72 different halftone patterns; and the blue curve is the error in the prediction of the mean central pixel absorptance by Model-45 $\times$ 45, and averaged over the 72 different halftone patterns. The results show that adding the correction weight term of the $45 \times 45 - 5 \times 5$ outer neighborhood can reduce the error significantly, which means that correction weight term of the Model-45$\times$45 can predict absorptance much more accurately than can the Model-5 $\times$ 5 alone. Finally, we conclude that the halftone pattern in the outer $45 \times 45 - 5 \times 5$ neighborhood can indeed have a significant influence on the central pixel absorptance.

5. CONCLUSION

In the present paper, we examine the potential influence of a much larger neighborhood (45$\times$45) on the absorptance value of the central pixel of the printed dot patterns. This model is an expansion of Mode-5$\times$5 which was proposed by Goyal et al in 2010.[13] We described a feasible strategy to estimate the $45 \times 45 - 5 \times 5$ neighborhood impact on the central pixel absorptance. The results show that the Model-45$\times$45 has the ability to better predict the absorptance value of printed dot patterns than other models.

REFERENCES

[1] Allebach, J. P., "Selected papers on digital halftoning," *SPIE Milestone Series* (1999).

[2] Baqai, F. A. and Allebach, J. P., "Halftoning via direct binary search using analytical and stochastic printer models," *IEEE Trans. Image Processing* **12**, 1–15 (Jan. 2003).

[3] Roetling, P. G. and Holladay, T. M., "Tone reproduction and screen design for pictorial electrographic printing," *J. Appl. Photo. Eng.* **15**, 179–182 (1979).

[4] Allebach, J. P., "Binary display of images when spot size exceeds step size," *Appl. Opt.* **19**, 2513–2519 (Aug. 1980).

[5] Stevenson, R. L. and Arce, G. R., "Binary display of hexagonally sampled continous-tone images," *J. Opt. Soc. Amer.* **2**, 1009–1013 (1985).

[6] Stucki, P., "Algorithms and procedures for digital halftone generation," *Proc. SPIE, Color Hardcopy, and Graphic Arts, J. Bares, Ed.* , 26–40 (1992).

[7] Rosenberg, C. J., "Measurement-based evaluation of a printer dot model for halftone algorithm tone correction," *J. Electronic Imaging* **2**, 205–212 (1993).

[8] Pappas, T. N., D. C. and Neuhoff, D. L., "Measurement of printer parameters for model-based halftoning," *J. Electronic Imaging* **2**, 193–204 (1993).

[9] Pappas, T. N. and Neuhoff, D. L., "Printer models and error diffusion," *IEEE Trans. Image Processing* **4**, 66–80 (1995).

[10] Lin, Q. and J.Wiseman, "Impact of electrophotographic printer dot modeling on halftone image quality," *SID Int. Symp. Tech. Papers, Seattle, WA* , 147150 (1993).

[11] Lin, Q., "Screen design for printing," *Proc. IEEE International Conference on Image Processing* (1995).

[12] Flohr, T. J. and Allebach, J. P., "Halftoning via direct binary search with a stochastic dot model," *Proc. IS&T's 3rd Tech. Symp. Prepress, Proofing, Printing, Chicago, IL* , 102–105 (1993).

[13] Goyal, P. and Gupta, M., "Electrophotographic model based halftoning," *Proc. SPIE, Color Imaging XV: Displaying, Processing, Hardcopy, and Applications* , 752810 (2010).

[14] Sezgin, M. and Sankur, B., "Survey over image thresholding techniques and quantitative performance evaluation," *Journal of Electronic Imaging* **13(1)**, 146–165 (Jan. 2004).